

Topological transport in Weyl semimetal

Banasree Sadhukhan

KTH Royal Institute of Technology, AlbaNova University Center, SE-10691, Stockholm, Sweden



I

Seminar at IISER Mohali, 3rd May, 2023



Swedish
Research
Council



"To be yourself in a world that is constantly trying to make you something else is the greatest accomplishment." —Ralph Waldo Emerson

Banasree Sadhukhan, PhD

✉ banasree.sadhukhan@gmail.com,
b.sadhukhan@ifw-dresden.de, banasree@kth.se

Education

PhD : **Condensed matter Physics** Presidency University 2018

Thesis title : "Study of electronic structure, optical and magnetic response of disordered solids"

M. Sc. : **Physics** University of Calcutta 2011

B. Sc. : **Physics** University of Calcutta 2009

Research Experience after PhD :

Researcher at KTH Royal institute of Technology, Stockholm, Sweden (September, 2022 - Present) (C)

Postdoctoral researcher at KTH Royal institute of Technology, Stockholm, Sweden (September, 2020 - August , 2022) (C)

Scientist at Institute for Solid State and Materials Research, IFW Dresden, Germany (March, 2019 - February, 2020) (B)

Postdoctoral researcher at Institute for Solid State and Materials Research, IFW Dresden, Germany (March, 2018 - February, 2019) (A)

Current research areas

Energy harvesting modern
(A) technologies

(B) Quantum materials and
Topological transport ★

Light-matter interaction
(C) in Skyrmion



Introduction and motivation

Topology, Weyl semimetal, symmetry



Theory and computation behind transport



Results and discussions on current research

Linear transport

[npj Quantum Materials 7, 19 \(2022\)](#) [Tunable chirality of noncentrosymmetric magnetic Weyl semimetals in rare-earth carbides]

[Phys. Rev. B 107 \(8\), L081110 \(2023\)](#) [Effect of chirality imbalances on Hall transport of PrRhC₂]

Non- Linear transport

[Phys. Rev. B 104, 245122 \(2021\)](#) [Electronic structure and unconventional nonlinear response in double Weyl semimetal SrSi₂]

[Phys. Rev. B 103, 144308 \(2021\)](#) [Role of time reversal symmetry and tilting in circular photogalvanic responses]



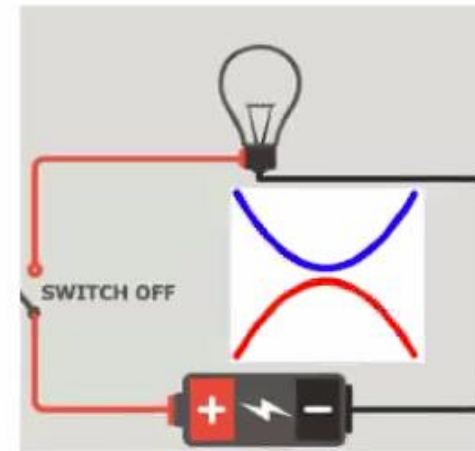
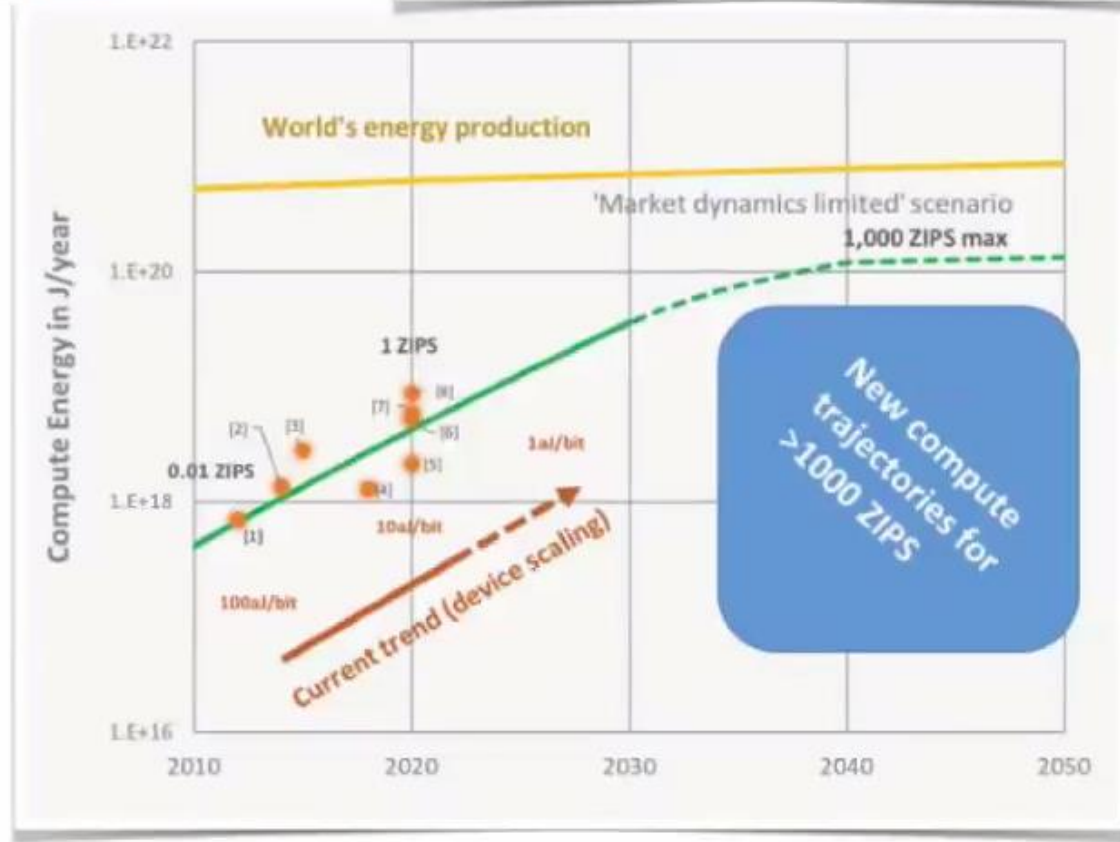
Conclusions



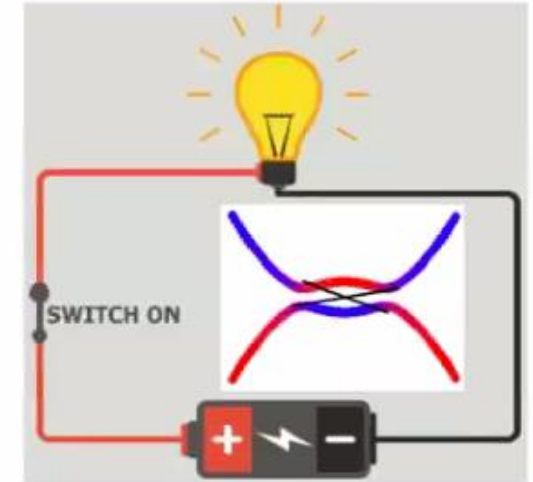
Published January 2021



Decadal Plan for Semiconductors FULL REPORT



Ordinary Insulator



Topological Insulator



New mechanisms for electronic conduction without dissipation at room temperature

- Need new technology with capacity to switch at lower energy than silicon device

- ★ Geometric properties (such as curvature) are local properties, but integral over local geometric properties give global topology



Gauss-Bonnet theorem for a closed surface

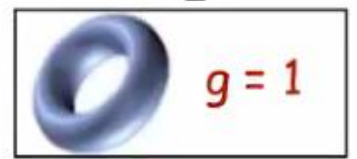
$$\frac{1}{2\pi} \int_S K da = \chi = 2 - 2g$$

Gaussian curvature

Genus (g)



$g = 0$



$g = 1$

- ★ Objects are described by topological invariants = Genus (g) of a surface = No of holes



David J. Thouless F. Duncan M. Haldane J. Michael Kosterlitz



The Nobel Prize in 2016

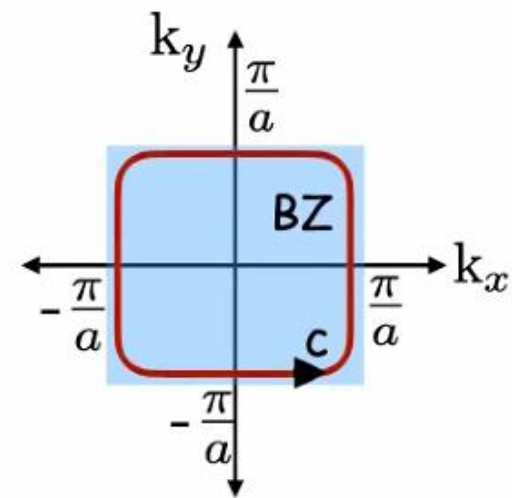
Quantized Hall effect in 2D electron gas
(Klaus von Klitzing, Nobel Laureate 1985)



TKNN Theory (1982) :

The Chern Insulator and the birth of "topological materials"

Bloch's theorem : $\psi_{\mathbf{k}}(\mathbf{r}) = e^{i\mathbf{k} \cdot \mathbf{r}} u_{\mathbf{k}}(\mathbf{r})$



Energy band can be characterized by a topological number

Berry phase : $e^{i\Phi_B(\Gamma)} = \exp \left(i \oint_{\Gamma} dk_a \mathcal{A}_n(\mathbf{k}) \right)$

Topological invariant : Chern number

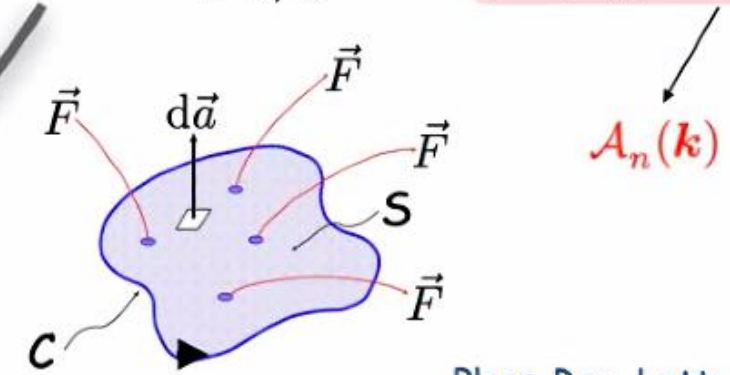
$$c_n = \frac{e^2}{h} \sum_{\text{occupied bands}} \int_{BZ} \frac{d^2 \mathbf{k}}{(2\pi)^2} F_n$$

$c_n = 0$
Normal insulator

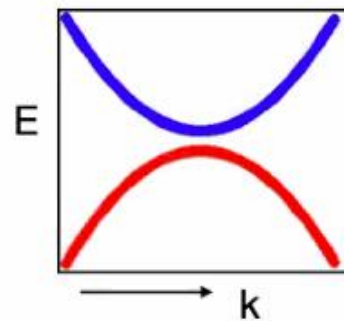
$c_n \neq 0$
Topological Chern insulator

Berry curvature

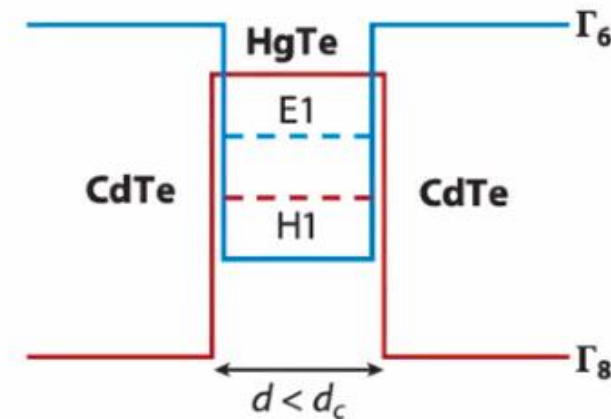
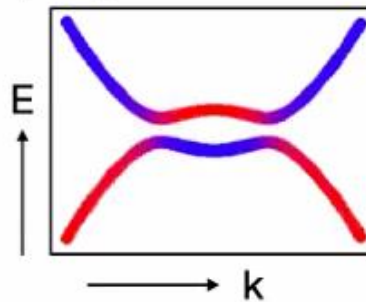
$$F_n = \sum_{l \neq n} \nabla_{\mathbf{k}} \times \langle u_n(\mathbf{k}) | i \nabla_{\mathbf{k}} | u_l(\mathbf{k}) \rangle$$



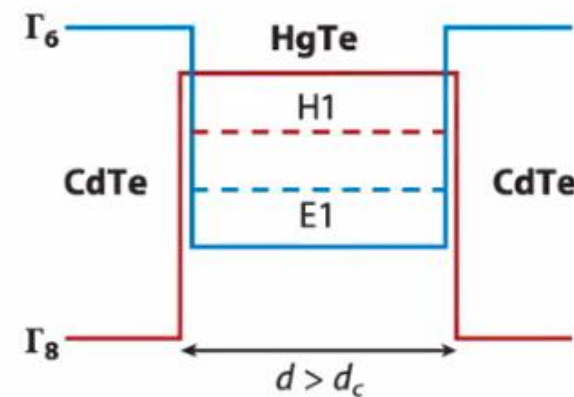
Normal insulator : CdTe



Topological insulator : HgTe



Trivial insulator :
 $E_{\Gamma_6} > E_{\Gamma_8}$

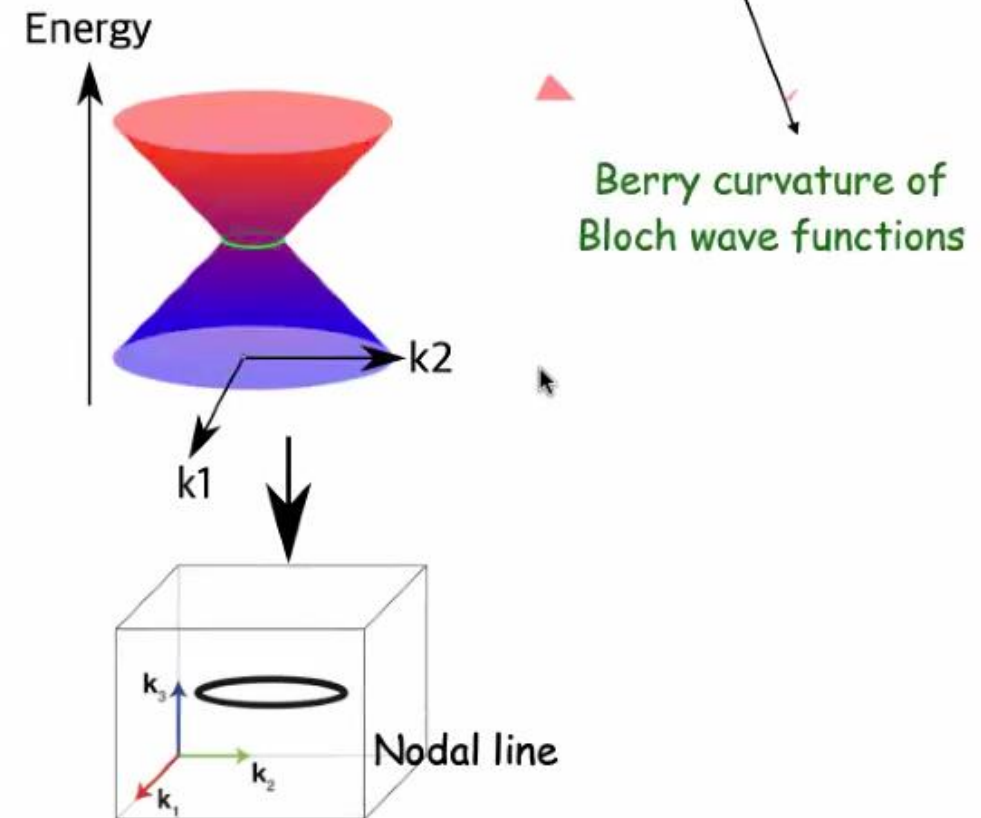
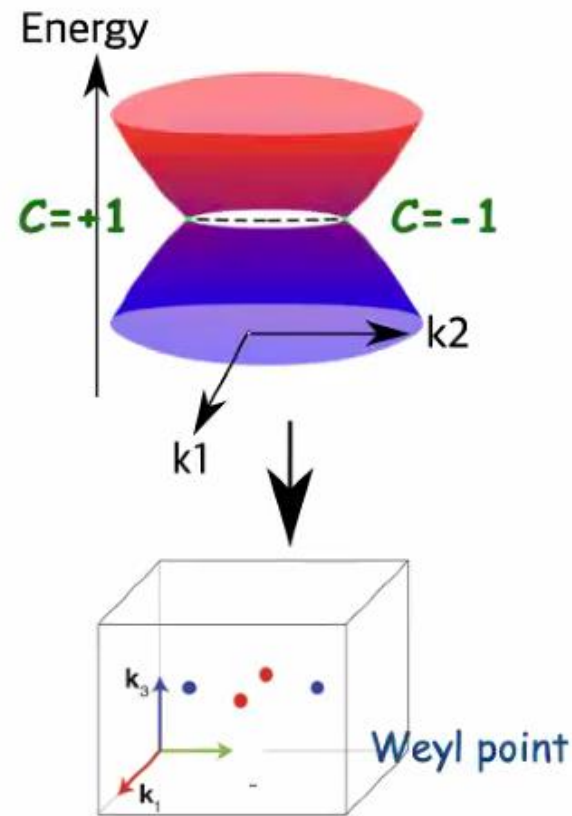
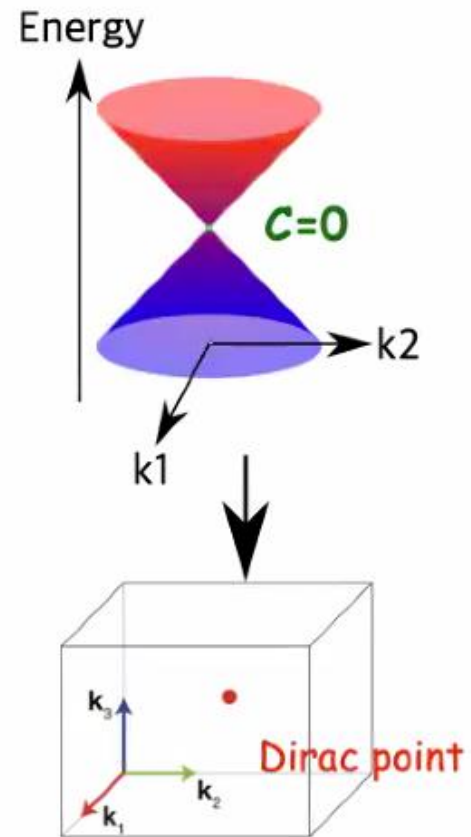


Nontrivial insulator :
 $E_{\Gamma_6} < E_{\Gamma_8}$

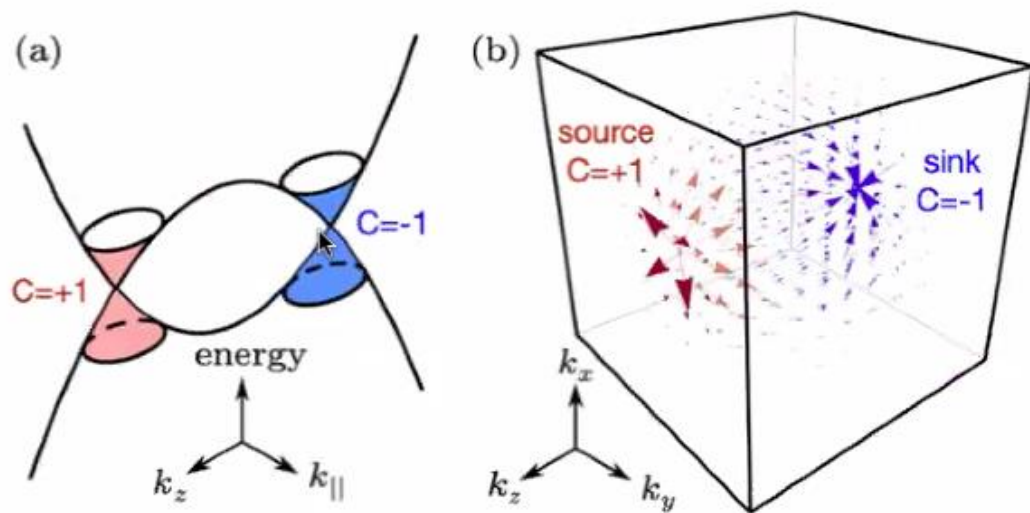
HgTe layer is thick and bands get inverted

Chern no (Topological invariant) : $C_n = \frac{1}{2\pi} \int_a dS \cdot \Omega_{nk}$

Dirac semimetal Weyl semimetal Nodal line semimetal

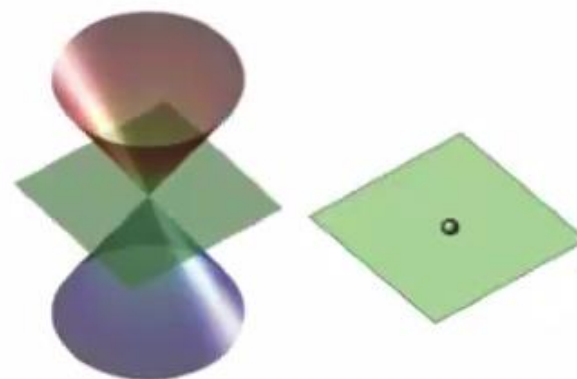


By breaking symmetries



Weyl point : Monopole of **Berry curvature**

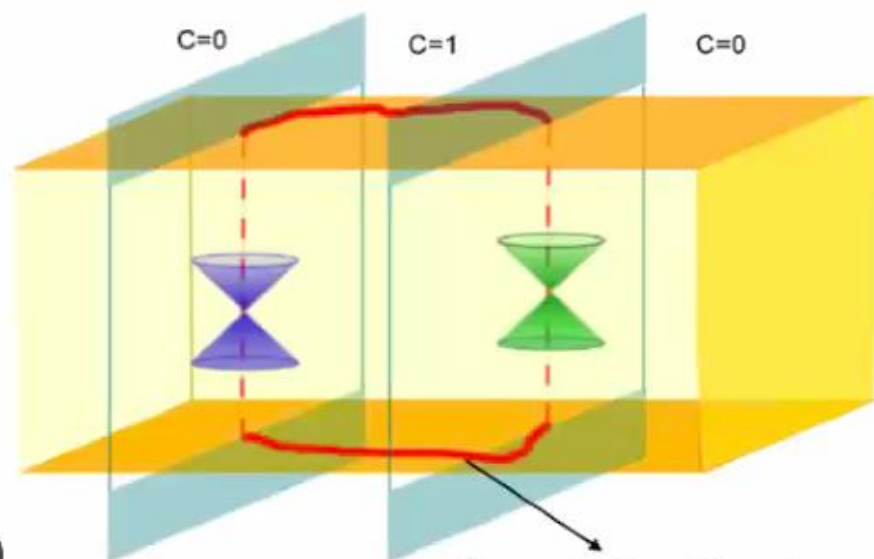
Low energy Weyl Hamiltonian : $H_{\text{Weyl}}(\mathbf{q}) = \hbar v_t q_t \sigma_0 + \hbar v_F \mathbf{q} \cdot \boldsymbol{\sigma}$



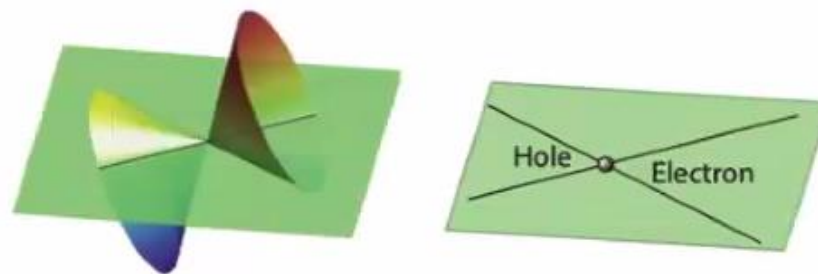
TaAs, TaP, NbAs, NbP

$$|v_t/v_f| < 1$$

Point like Fermi surface



Surface state : Fermi arc

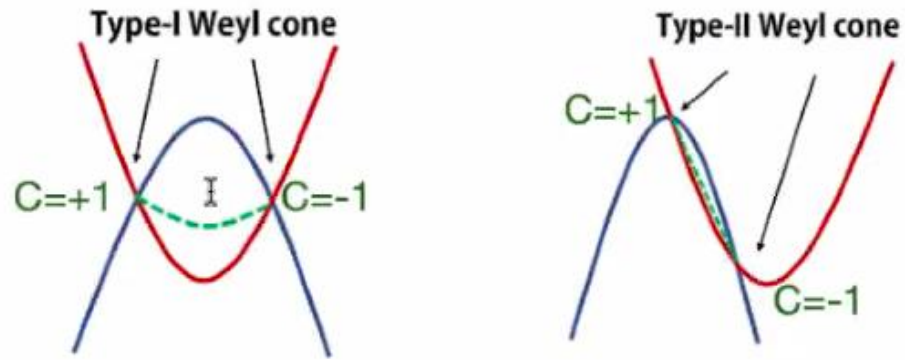


MoTe2, WTe2

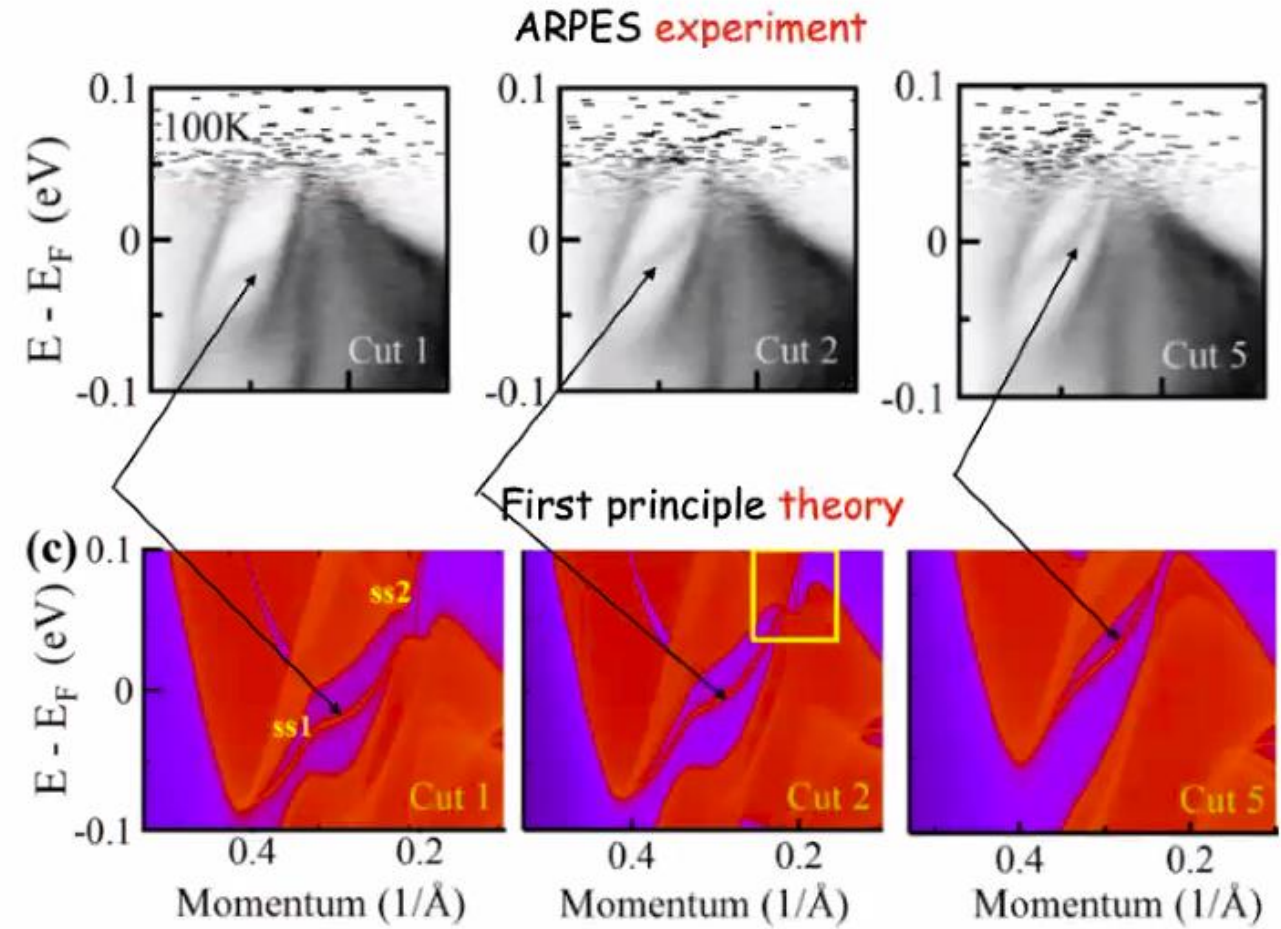
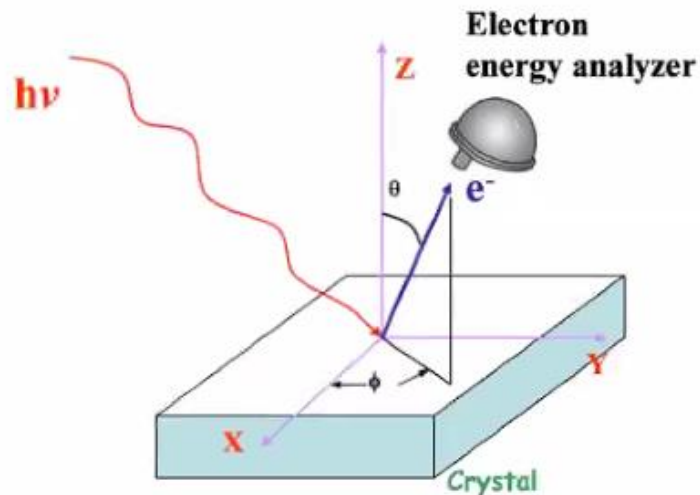
$$|v_t/v_f| > 1$$

Pocket like Fermi surface

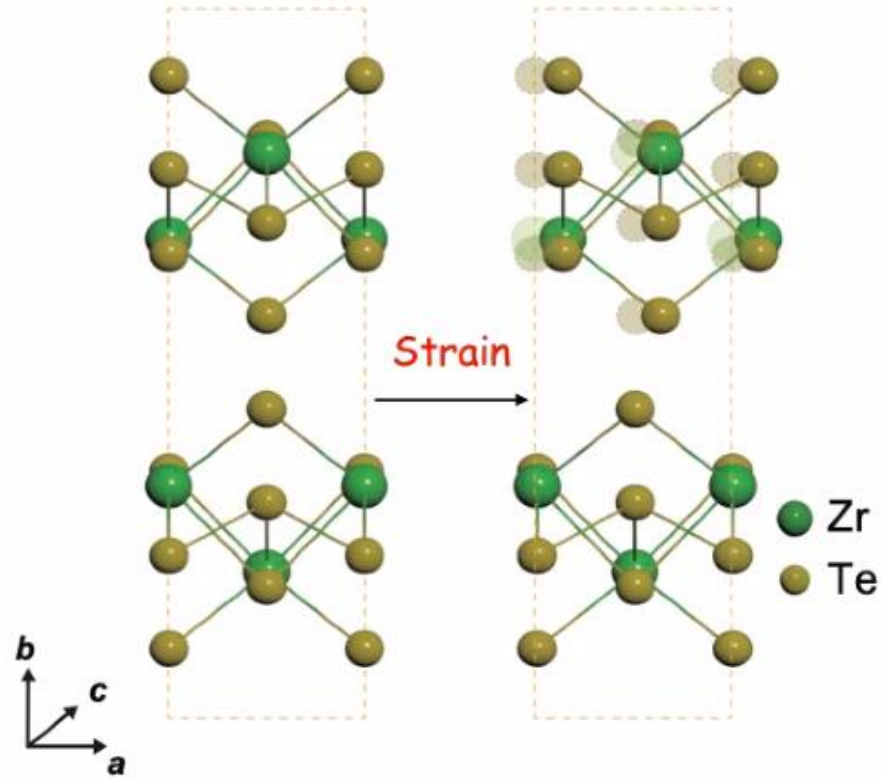
Type-II Weyl semimetal **WTe₂**



Experimental setup for ARPES



Inversion symmetry ($x \rightarrow -x, y \rightarrow -y, z \rightarrow -z$)

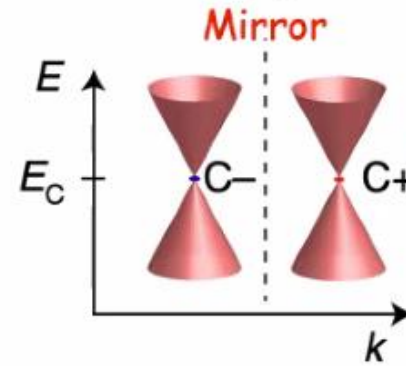


Dirac semimetal : ZrTe_5

Dirac point



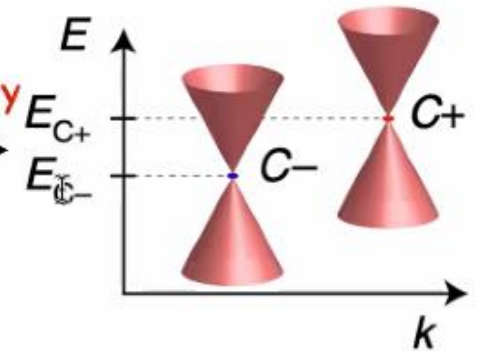
Breaking of inversion symmetry



Degenerated Weyl point

Weyl Semimetals like TaAs , MoTe_2

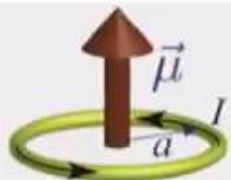
Break mirror symmetry



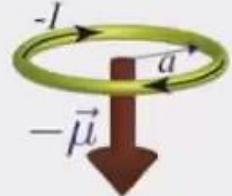
Non-degenerated Weyl point

CoSi , RhSi , SrSi_2

Time reversal symmetry →

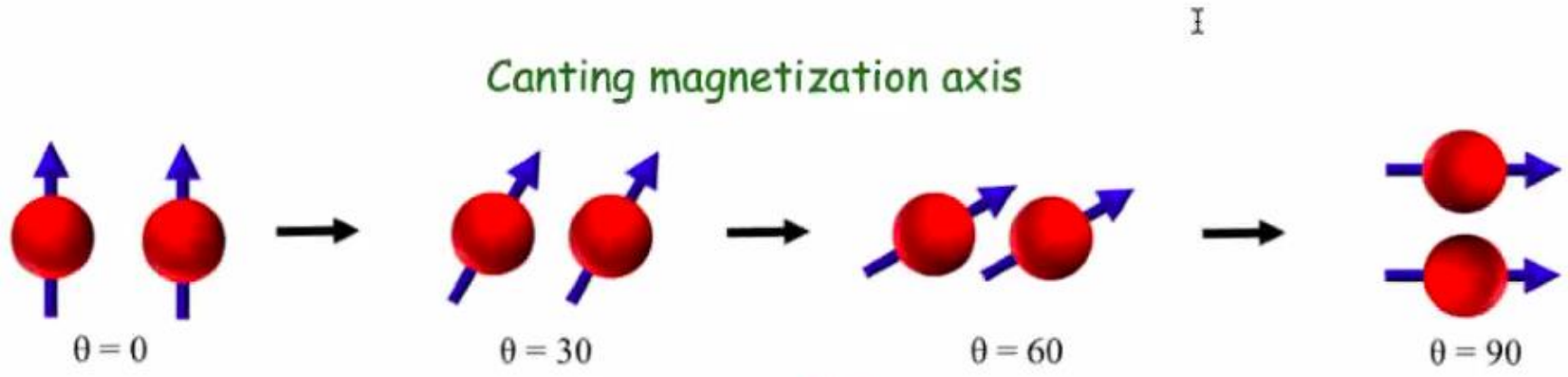
Classical Picture:  $\vec{\mu} = \frac{\pi I a^2}{c} \hat{z}$

And, applying the time-reversal operator:

$$\hat{T} I = -I \rightarrow \hat{T} \vec{\mu} = -\vec{\mu}$$


Which is the same as applying $\hat{T} = i\sigma^y \hat{K}$ to the spin.

Therefore, for a ferromagnet:

$$\hat{T} \{ \uparrow \uparrow \uparrow \uparrow \uparrow \uparrow \uparrow \uparrow \} = \downarrow \downarrow \downarrow \downarrow \downarrow \downarrow \downarrow \downarrow$$


The semiclassical equations of motion
 $\sqrt{B} \ll \mu$

$$\dot{\mathbf{r}} = D(\mathbf{B}, \boldsymbol{\Omega}_{\mathbf{k}}) [\mathbf{v}_{\mathbf{k}} + \underbrace{e(\mathbf{E} \times \boldsymbol{\Omega}_{\mathbf{k}})}_{\text{AV}} + \underbrace{e(\mathbf{v}_{\mathbf{k}} \cdot \boldsymbol{\Omega}_{\mathbf{k}})\mathbf{B}}_{\text{CME}}],$$

$$\dot{\mathbf{k}} = D(\mathbf{B}, \boldsymbol{\Omega}_{\mathbf{k}}) [e\mathbf{E} + e(\mathbf{v}_{\mathbf{k}} \times \mathbf{B}) + \underbrace{e^2(\mathbf{E} \cdot \mathbf{B})\boldsymbol{\Omega}_{\mathbf{k}}}_{\text{CA}}]$$

• Charge current $\mathbf{J} = \int \frac{d^3k}{(2\pi)^3} D\dot{\mathbf{r}} f_{\mathbf{k},\mathbf{r},t}$

$$\mathbf{J} = \mathbf{J}_D + \mathbf{J}_{\text{AH}} + \mathbf{J}_{\text{CA/CME}}$$

Drift current

Anomalous Hall current

Chiral current

For CA : $(\mathbf{B} \cdot \mathbf{E})$

For CME : $\mathbf{E} = 0$

$$\mathbf{J}_D \approx \int \frac{d^3k}{(2\pi)^3} \mathbf{v}_{\mathbf{k}} f_{\mathbf{k},\mathbf{r},t}$$

$$\mathbf{J}_{\text{AH}} \approx \mathbf{E} \times \int \frac{d^3k}{(2\pi)^3} \boldsymbol{\Omega}_{\mathbf{k}} f_{\mathbf{k},\mathbf{r},t}$$

Berry curvature

$$\mathbf{J}_{\text{CA/CME}} \approx \mathbf{B} \int \frac{d^3k}{(2\pi)^3} (\mathbf{v}_{\mathbf{k}} \cdot \boldsymbol{\Omega}_{\mathbf{k}}) f_{\mathbf{k},\mathbf{r},t}$$

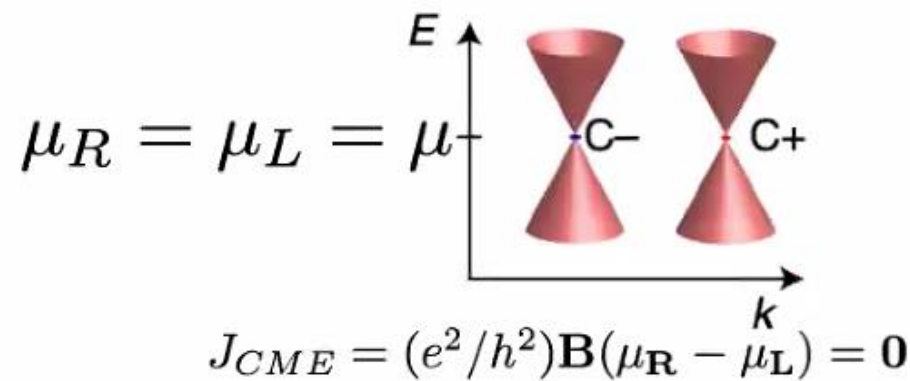
Chiral contribution

(E, B)
$$\mathbf{J}_D \approx \int \frac{d^3 k}{(2\pi)^3} \mathbf{v}_k f_{\mathbf{k}, \mathbf{r}, t}$$
$$\mathbf{J}_{\text{AH}} \approx \mathbf{E} \times \int \frac{d^3 k}{(2\pi)^3} \boldsymbol{\Omega}_{\mathbf{k}} f_{\mathbf{k},\mathbf{r},t}$$
$$\mathbf{J}_{\text{CA/CME}} \approx \mathbf{B} \int \frac{d^3 k}{(2\pi)^3} (\mathbf{v}_{\mathbf{k}} \cdot \boldsymbol{\Omega}_{\mathbf{k}}) f_{\mathbf{k},r,t}$$

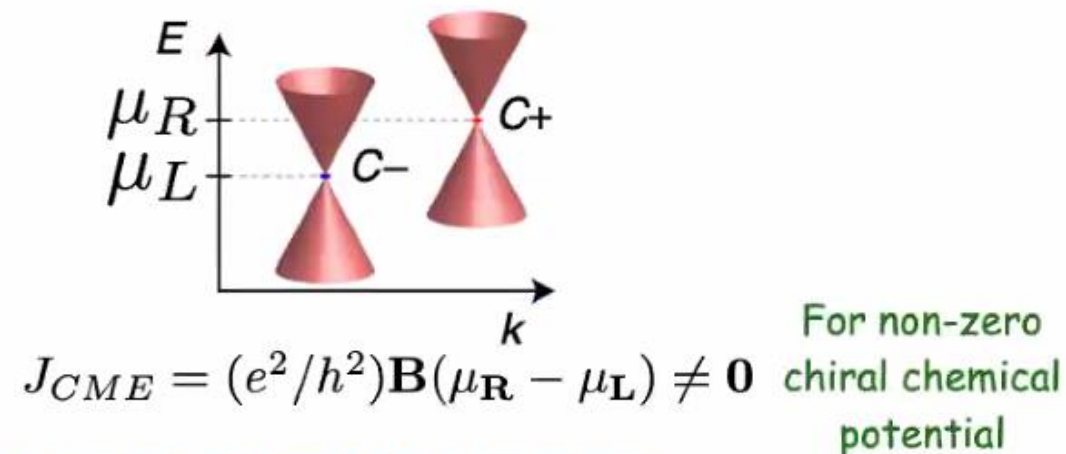
"Chiral magnetic effect" works if Weyl points appear at different energy levels.

- Fermi surface integral and integrating by parts for the term $f_{\mathbf{k}n} (\mathbf{v}_{\mathbf{k}n} \cdot \boldsymbol{\Omega}_{\mathbf{k}n})$ and putting $\frac{\delta f^0}{\delta \mathbf{k}} = -\hat{\mathbf{v}}_{\mathbf{f}} \delta^3(\mathbf{k} - \mathbf{k}_f)$ with $\hat{\mathbf{v}}_{\mathbf{f}}$ the FS normal at \mathbf{k}_f , and introduce the Chern number $C_{na} = (1/2\pi) \int_{S_{na}} dS (\hat{\mathbf{v}}_F \cdot \boldsymbol{\Omega}_{\mathbf{k}n})$ of the a th Fermi sheet S_{na} in band n

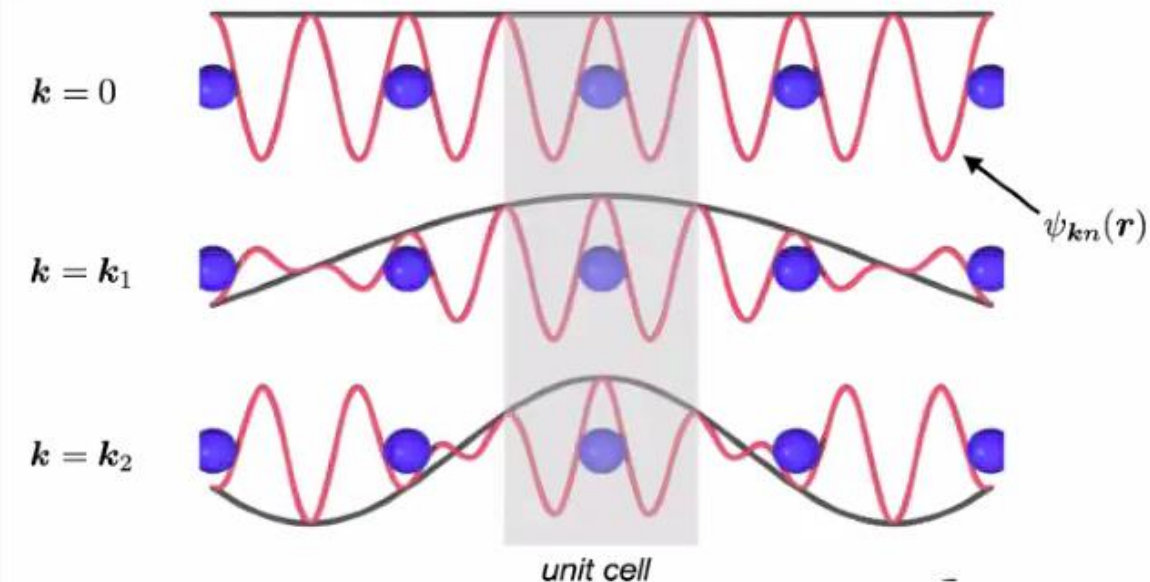
- For $\mathbf{E} = \mathbf{0}$, chiral magnetic effect (CME) : $J_{CME} = -\frac{e^2}{\hbar^2} \sum_{m\alpha} \mu_{m\alpha} C_{m\alpha}$



Chiral chemical
potential =
 $\mu_R - \mu_L$



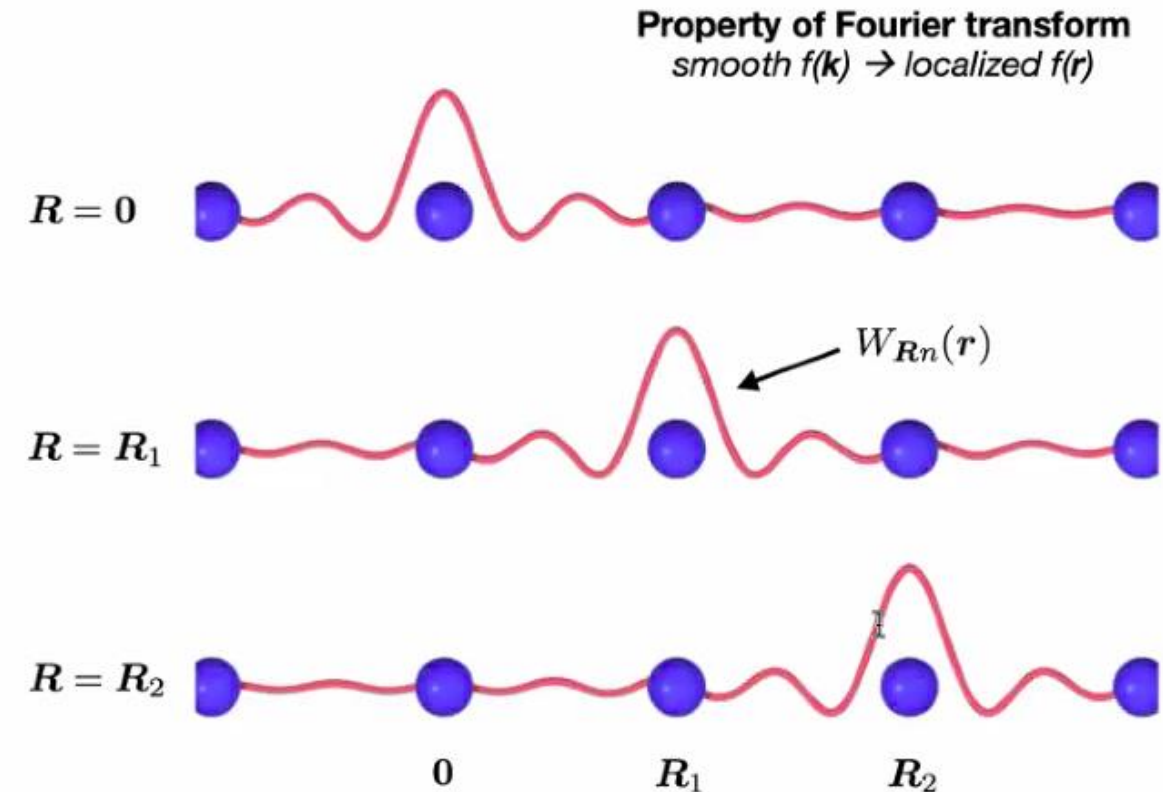
Bloch wave functions : $\psi_{\mathbf{k}n}(\mathbf{r}) = e^{i\mathbf{k}\cdot\mathbf{r}} u_{\mathbf{k}n}(\mathbf{r})$



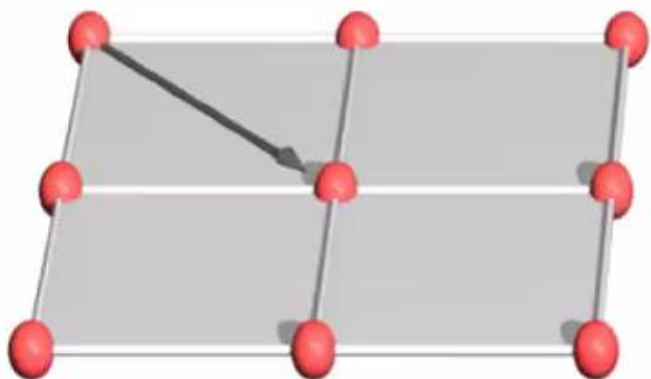
- Bloch functions are **extended and delocalized**

- **Localized** wave functions in real space offer more microscopic insights into the underlying physics.

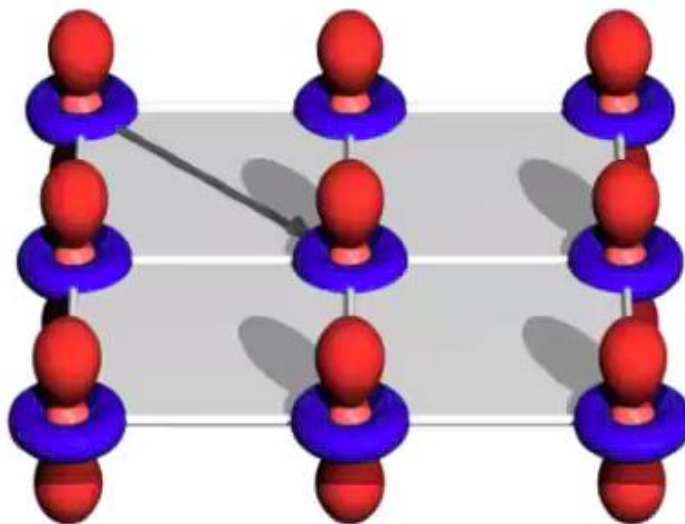
Wannier function : $W_{Rn}(\mathbf{r}) = \frac{1}{N} \sum_{\mathbf{k}} e^{-i\mathbf{k}\cdot\mathbf{R}} \psi_{\mathbf{k}n}(\mathbf{r})$



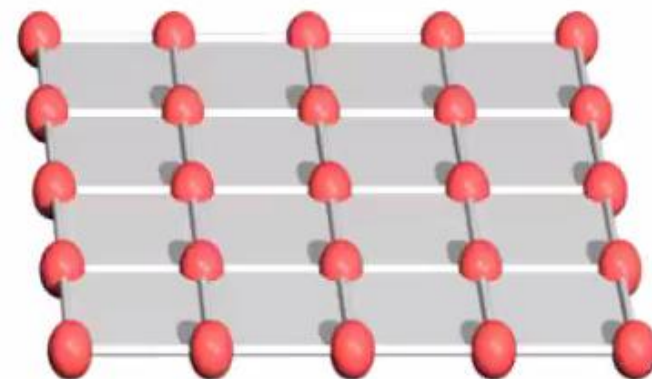
$H(\mathbf{k})$



$H(\mathbf{R})$



$H(\mathbf{q})$



(Developed transport code)

*DFT on coarse mesh
(e.g., 8^3 \mathbf{k} -points)*



DFT packages : VASP, FPLO,
WIEN2K, Quantum Espresso

*maximally localized
Wannier functions*



$$H = \sum_{\mathbf{R}\mathbf{R}'} \sum_{nn'} t_{nn'}(\mathbf{R}, \mathbf{R}') |W_{\mathbf{R}n}\rangle \langle W_{\mathbf{R}'n'}|$$



Berry curvature,
Transport

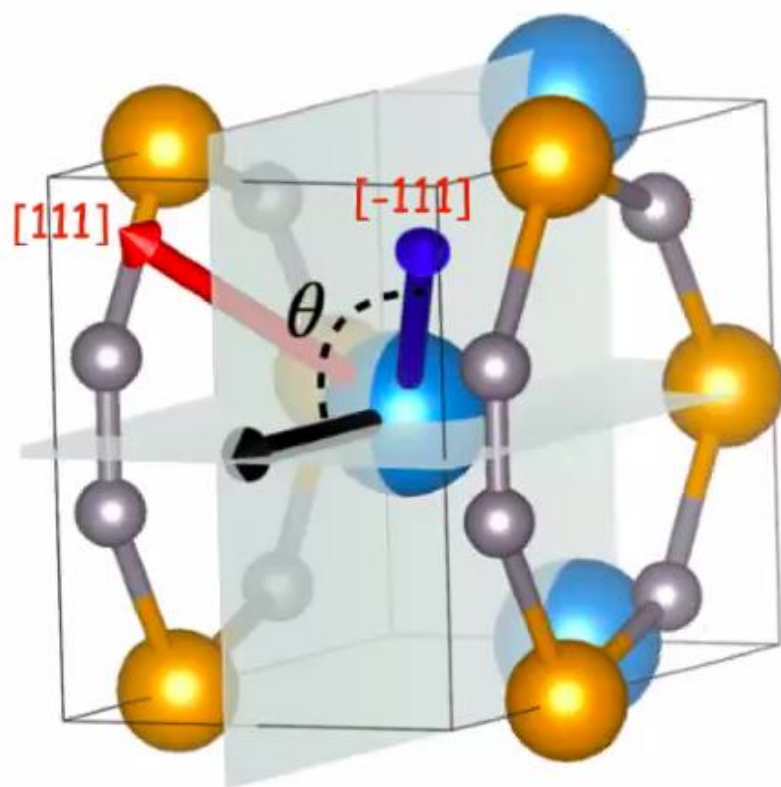
R. Ray,, B. Sadhukhan et al. npj Quantum Materials 7, 19 (2022)

Crystal symmetry : $\{E, m(x), m(y), C2(z)\}$

$m(x)$: mirror along x

$m(y)$: mirror along y

$C2(z)$: rotation along z



T is time reversal symmetry

Magnetization axis

Symmetry

Degeneracy of
Weyl nodes

Principle axis say,
[001]

$\{E, m(x)T, m(y)T, C2(z)\}$

4

Face diagonal say,
[011]

$\{E, m(x)T\}$

2

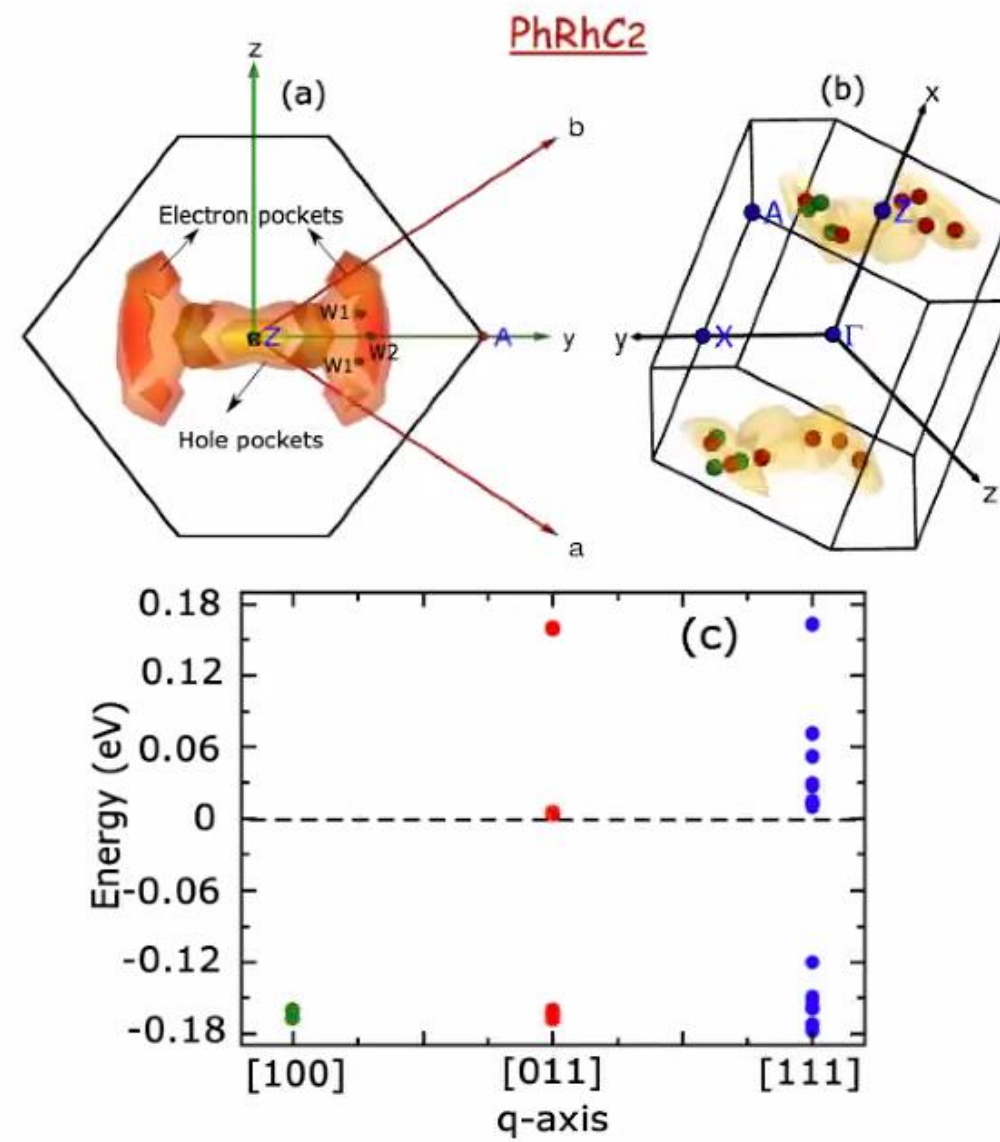
Body diagonal say,
[111]

$\{E\}$

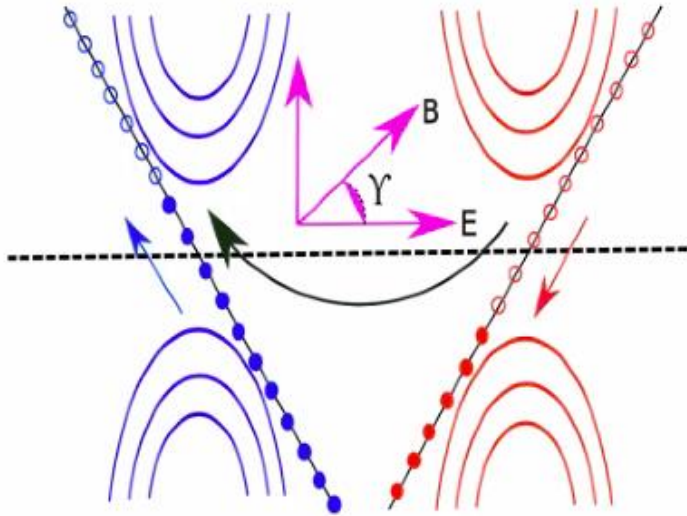
1

Breaks all symmetries

All Weyl nodes are non-degenerate



What is chiral anomaly?

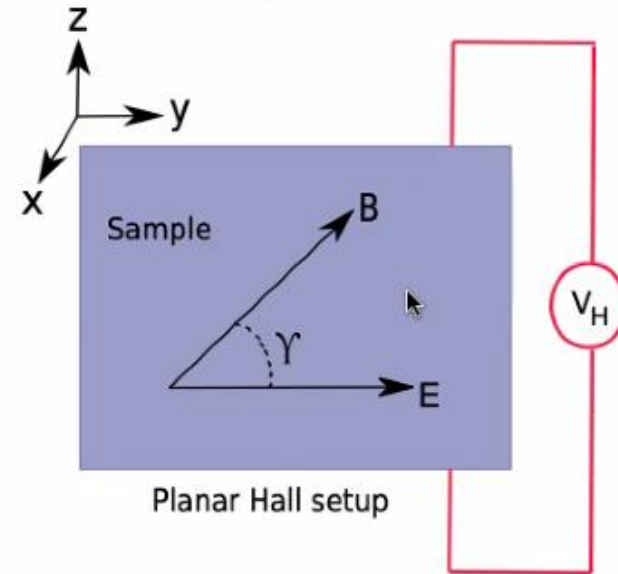


Chiral anomaly ($\mathbf{E} \cdot \mathbf{B}$)

Continuity equation: $\frac{\partial n_i}{\partial t} + \nabla \cdot \mathbf{J}_i = \frac{C_i}{4\pi^2} \mathbf{B} \cdot \mathbf{E}$

Phys. Rev. Lett. **109**, 181602 (2012)

Phys. Rev. Lett. **119**, 176804 (2017)



$$T \ll \sqrt{B} \ll \mu \quad \mathbf{B} = B \cos \gamma \hat{y} + B \sin \gamma \hat{z}, \quad \mathbf{E} = E \hat{y}$$

$$\sigma_{zy} \simeq e^2 \int \frac{d^3 k}{(2\pi)^3} D\tau \left(-\frac{\partial f_0}{\partial \epsilon} \right) \left[\left(v_z + \frac{eB \sin \gamma}{\hbar} (\boldsymbol{\Omega}_{\mathbf{k}} \cdot \mathbf{v}_{\mathbf{k}}) \right) \right. \\ \left. \left(v_y + \frac{eB \cos \gamma}{\hbar} (\boldsymbol{\Omega}_{\mathbf{k}} \cdot \mathbf{v}_{\mathbf{k}}) \right) \right]$$

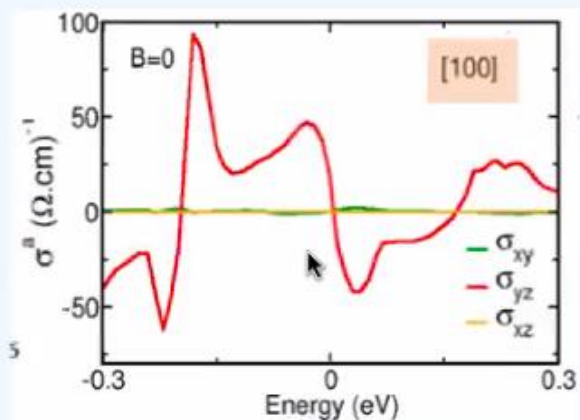
Planar Hall conductivity

$$\sigma_{zy} \propto \sin \gamma \cos \gamma$$

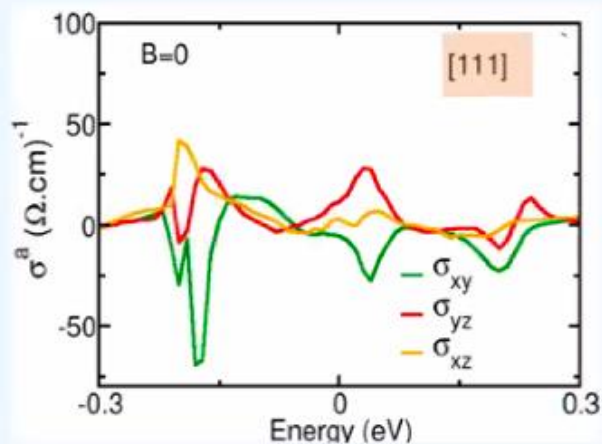
Longitudinal magneto conductivity

$$\sigma_{yy} \propto \cos^2 \gamma$$

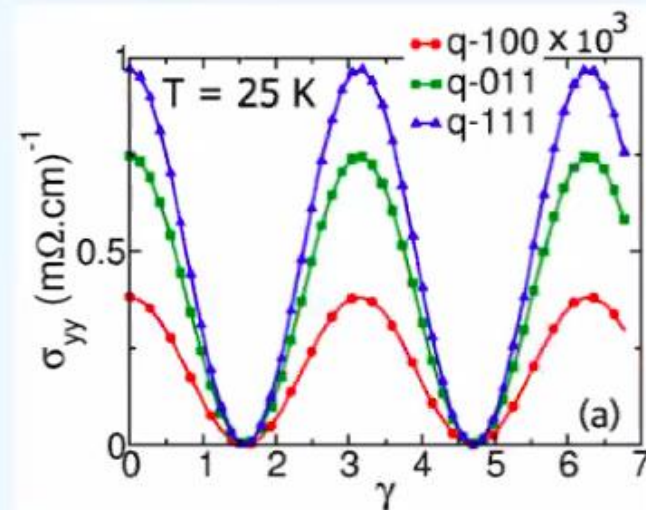
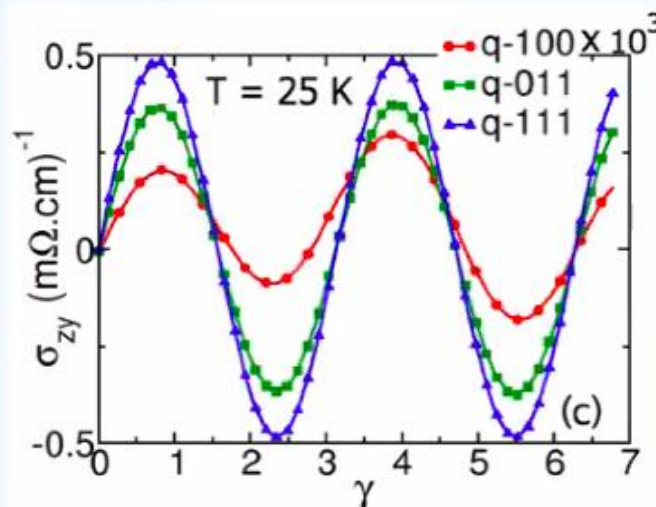
Anomalous Hall effect (B=0)



Higher to lower
symmetry



Planar Hall effect (B ≠ 0)

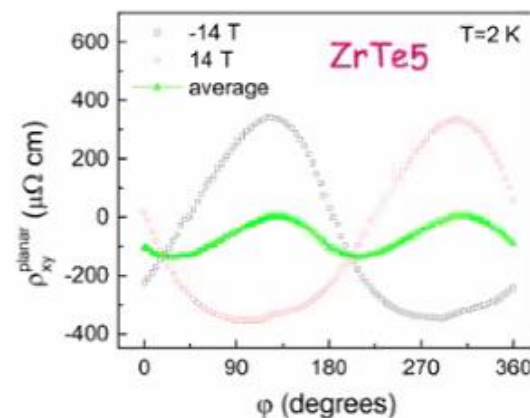


B. Sadhukhan et al. Phys. Rev. B 107 (8), L081110 (2023)

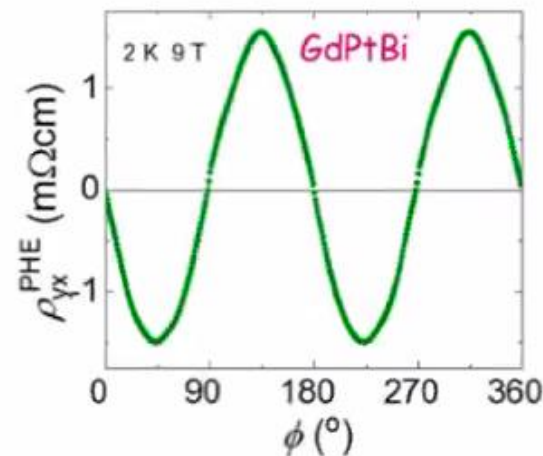
Experimental findings from other groups

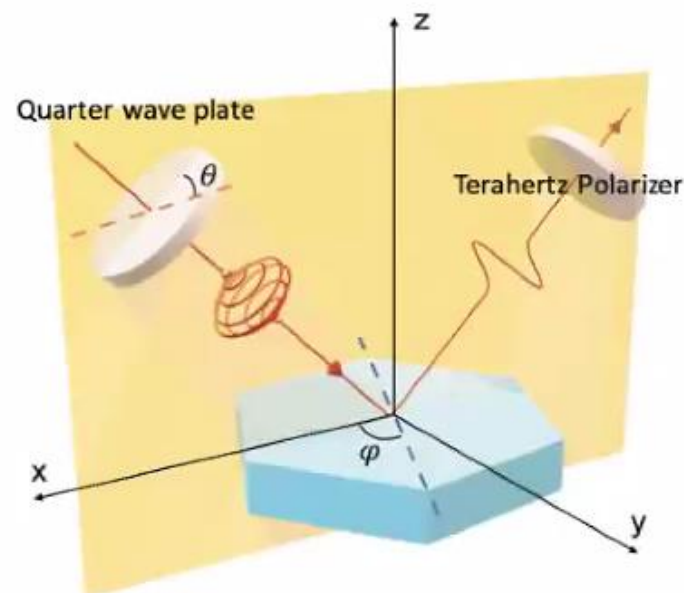


Phys. Rev. B 98, 121108(R) (2018)



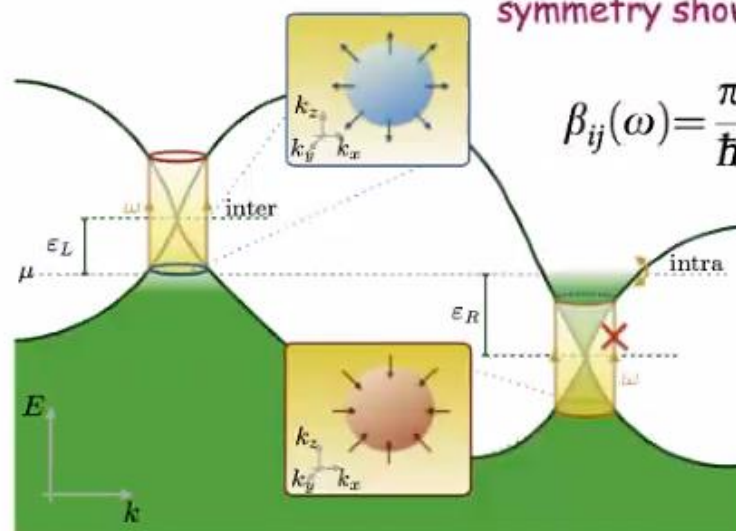
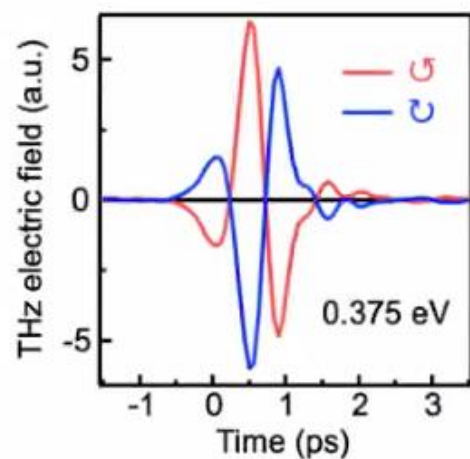
Phys. Rev. B 98, 041103(R) (2018)





$$\frac{dJ_a}{dt} = \beta_{ab}(\omega) [\mathbf{E}(\omega) \times \mathbf{E}^*(\omega)]_b$$

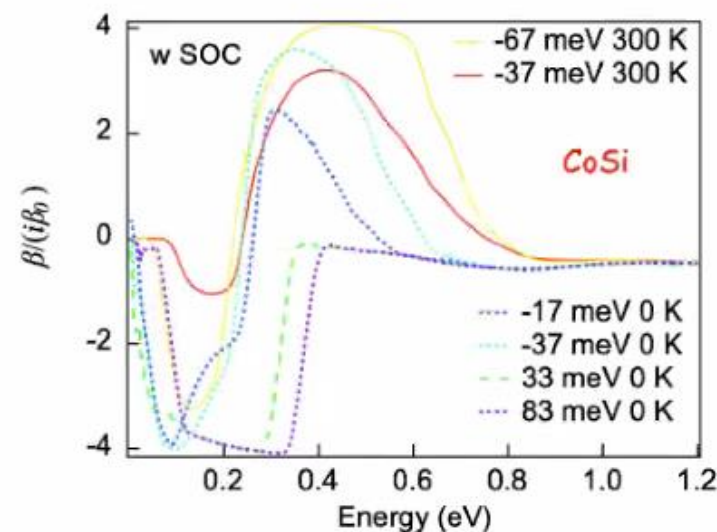
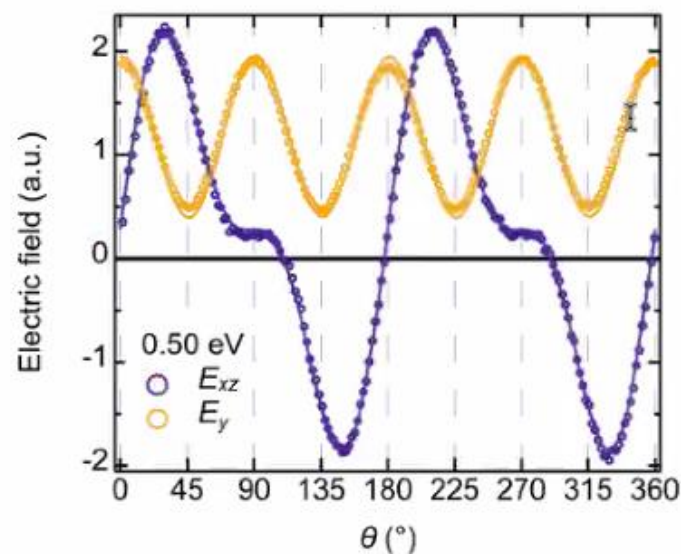
CPG tensor



$$\beta_{ij}(\omega) = \frac{\pi e^3}{\hbar V} \epsilon_{jkl} \sum_{\mathbf{k}, n, m} f_{nm}^{\mathbf{k}} \Delta_{\mathbf{k}, nm}^i r_{\mathbf{k}, nm}^k r_{\mathbf{k}, mn}^l \delta(\hbar\omega - E_{\mathbf{k}, mn})$$

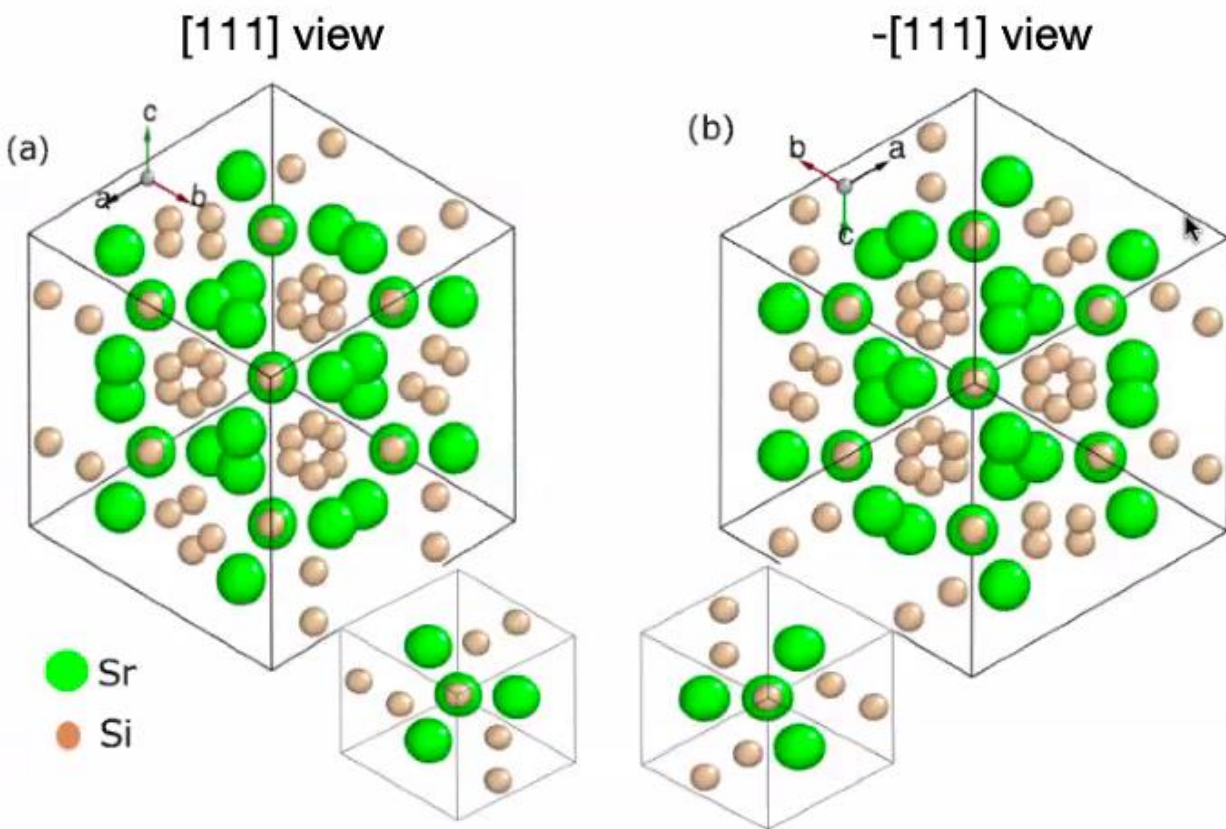
$$\text{Tr}[\beta(\omega)] = i\pi \frac{e^3}{h^2} C_L \equiv i\beta_0$$

- Nat. Commun. **8**, 15995 (2017)

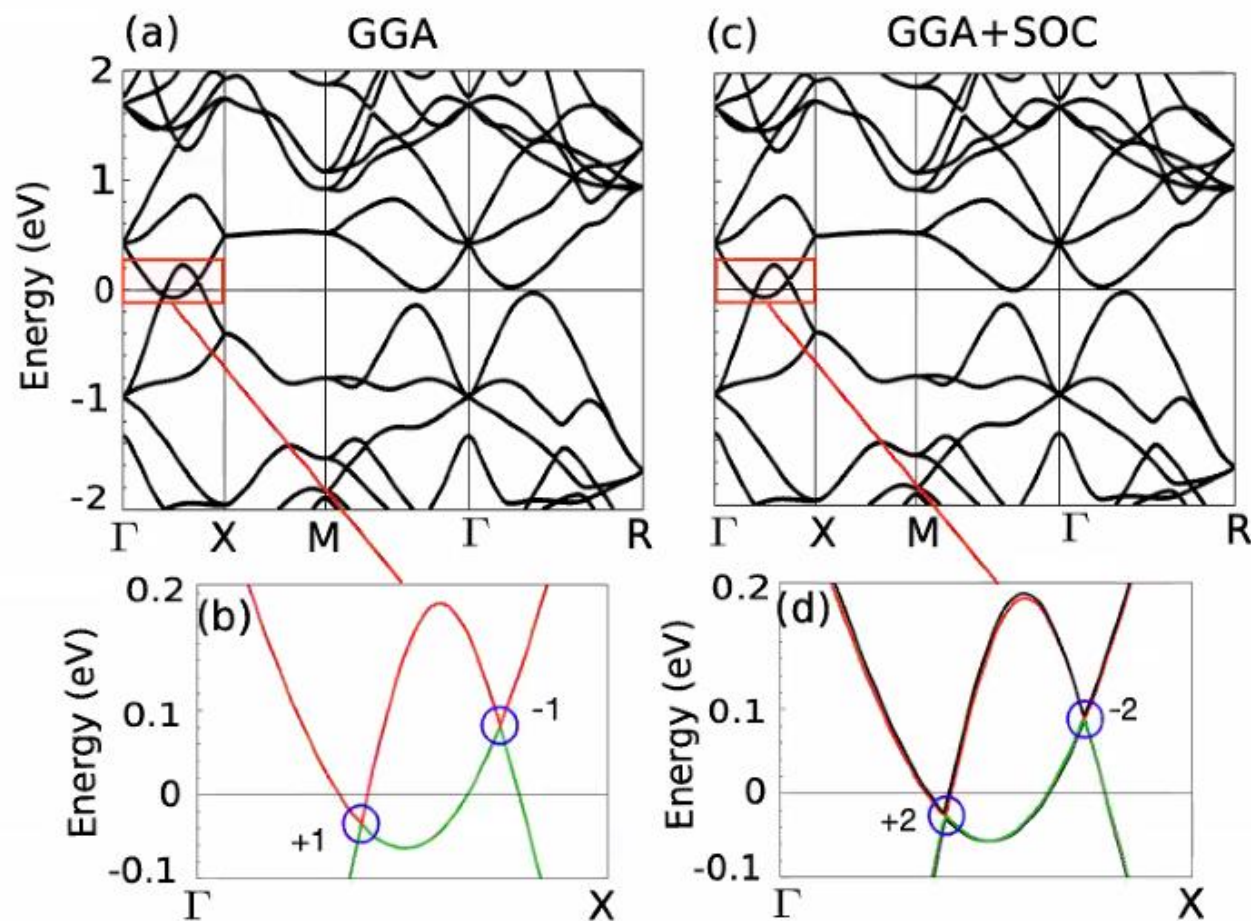


Some experimental findings from other group
(Nature Communications **12**, 154 (2021))

Space group $P4332 (212)$ with the lattice constant 6.563 \AA



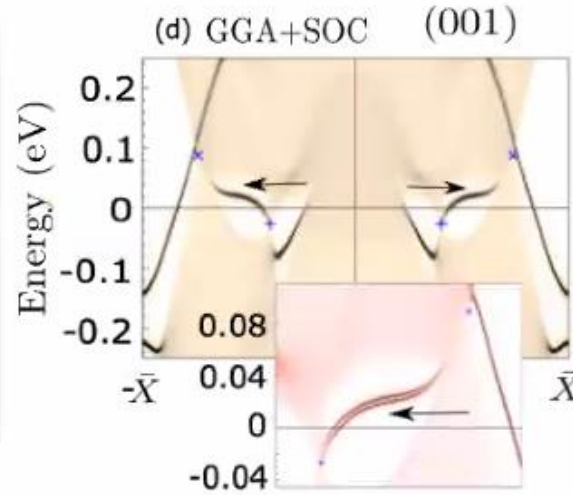
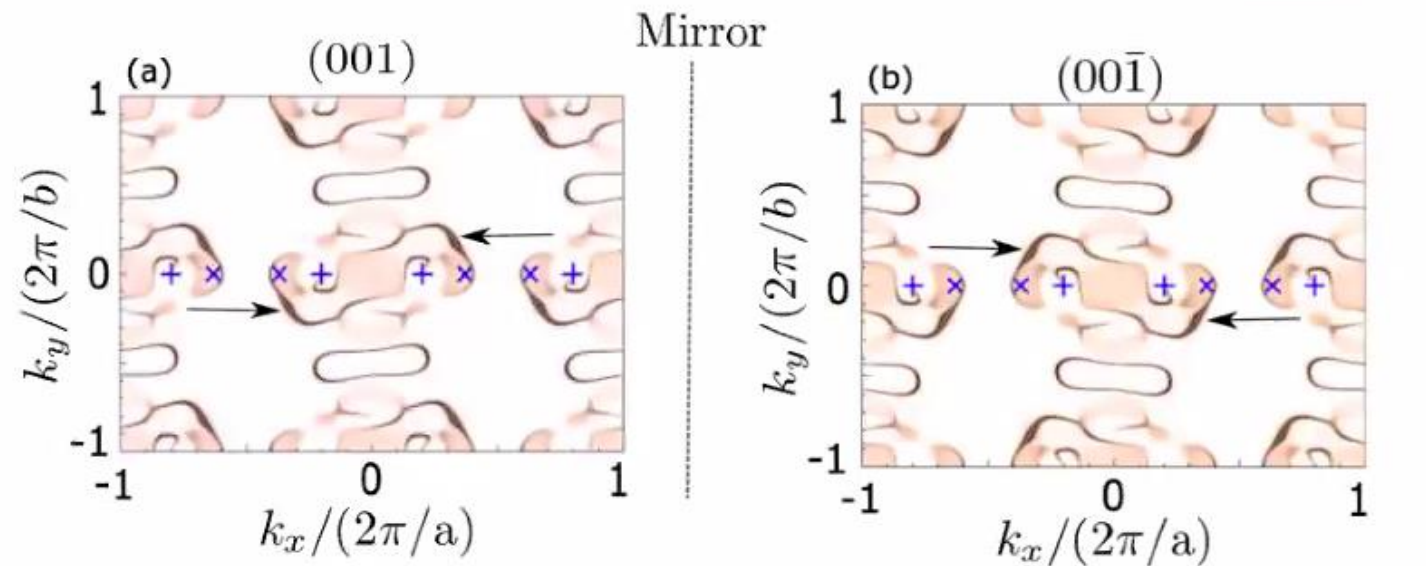
$-[111]$ view is mirror+flipped view of $[111]$. Structural chirality generates a distinct handedness which affect topological properties



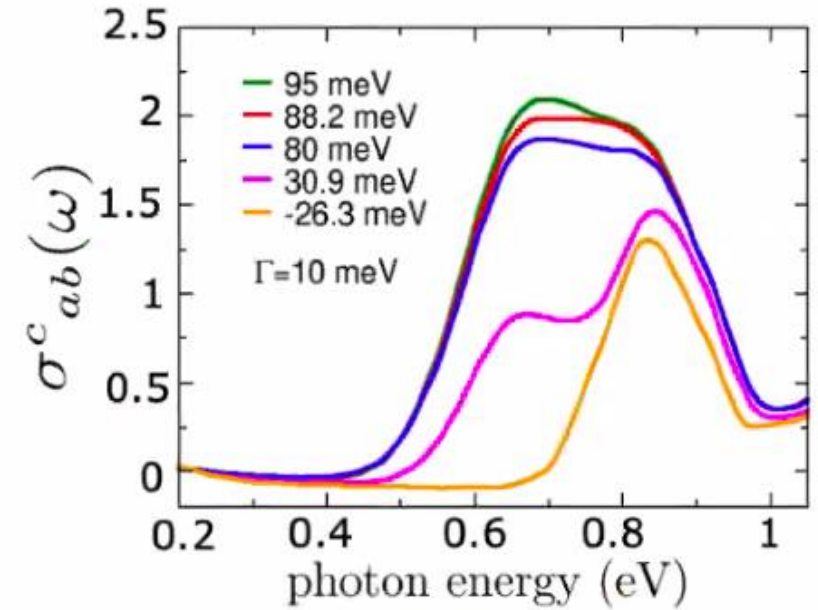
Chiral WSM SrSi_2 = Breaking of (Inversion+mirror) symmetries

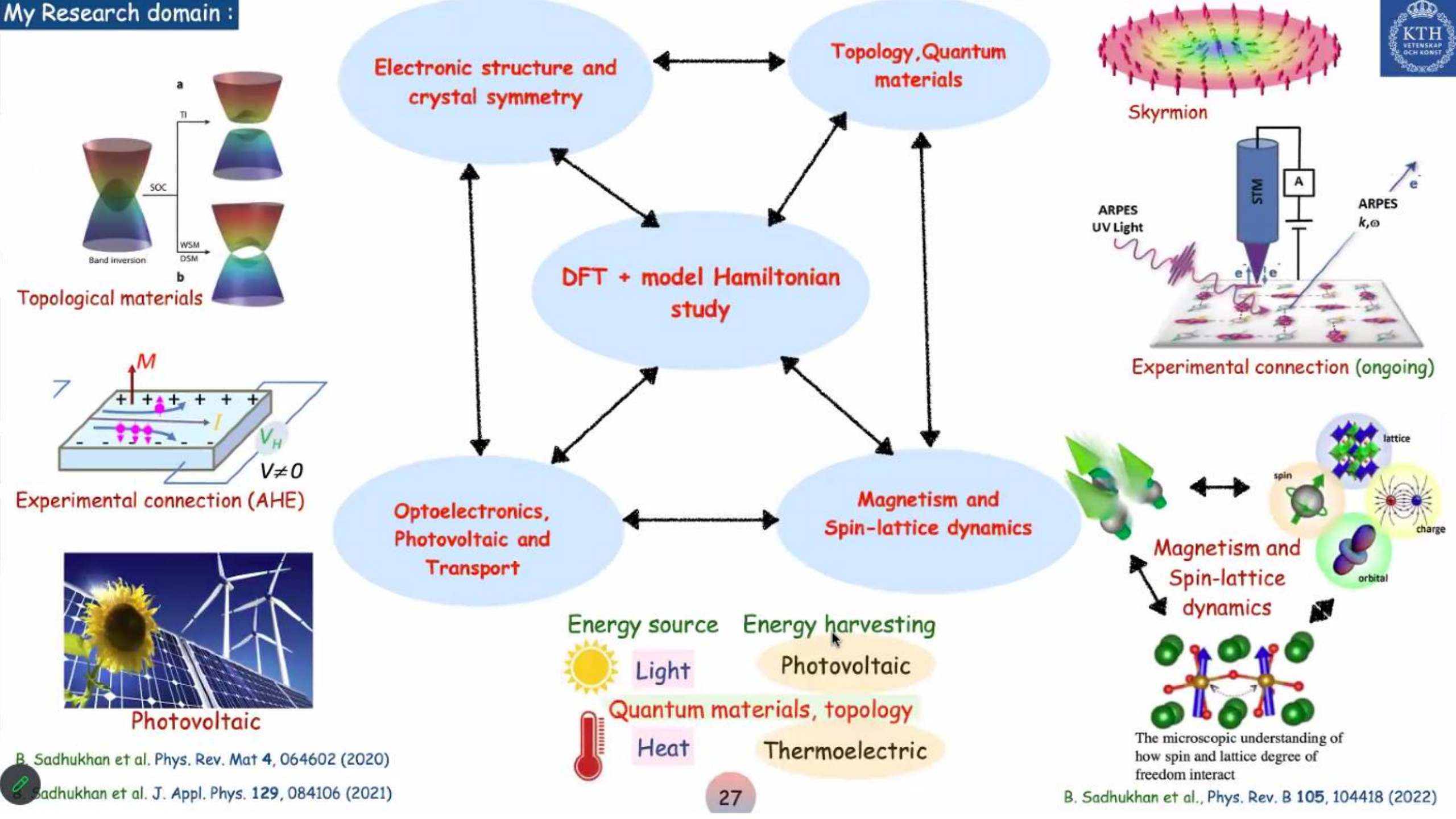
TABLE I. Positions, Chern numbers, and energies of the WNs with SOC ($W_{1,2}$) and without SOC ($V_{1,2}$).

WP	Position $[(k_x, k_y, k_z)]$ in $(\frac{2\pi}{a}, \frac{2\pi}{b}, \frac{2\pi}{c})$	C	E (meV)
V_1	$(\pm 0.2001, 0, 0)$	+1	-34.4
V_2	$(\pm 0.3691, 0, 0)$	-1	82.3
W_1	$(\pm 0.2003, 0, 0)$	+2	-26.3
W_2	$(\pm 0.3696, 0, 0)$	-2	88.2



$$\sigma_{ab}^c(\omega) = \frac{e^3}{\omega^2} \text{Re} \left\{ \phi_{ab} \sum_{\Omega=\pm\omega} \sum_{l,m,n} \int_{BZ} \frac{d^3k}{(2\pi)^3} (f_l^{\vec{k}} - f_n^{\vec{k}}) \right. \\ \left. \times \frac{\langle n_{\vec{k}} | \hat{v}_a | l_{\vec{k}} \rangle \langle l_{\vec{k}} | \hat{v}_b | m_{\vec{k}} \rangle \langle m_{\vec{k}} | \hat{v}_c | n_{\vec{k}} \rangle}{(E_{\vec{k}n} - E_{\vec{k}m} - i\Gamma)(E_{\vec{k}n} - E_{\vec{k}l} - \hbar\Omega - i\Gamma)} \right\} \\ \approx iC\beta_0\tau$$





Quantum materials and topological transport

- (1) "Effect of chirality imbalance on Hall transport of PrRhC_2 " B. Sadhukhan, T. Nag, Physical Review B **107** (8), L081110 (2023)
- (2) "Tunable chirality of noncentrosymmetric magnetic Weyl semimetals in rare-earth carbides" R. Ray, B. Sadhukhan, M. Richter, J.I. Facio, J. van den Brink, npj Quantum Materials **7**, 19 (2022)
- (3) "Electronic structure and unconventional nonlinear response in double Weyl semimetal SrSi_2 " B. Sadhukhan, T. Nag Phys. Rev. B **104**, 245122 (2021)
- (4) "Role of time reversal symmetry and tilting in circular photogalvanic responses" B. Sadhukhan, T. Nag Phys. Rev. B **103**, 144308 (2021)

Bulk Photovoltaic and sustainable energy

- (1) "A new topological quantum material ZnGeSb_2 with pressure-driven tunable properties in chalcopyrite series" S. Sadhukhan, B. Sadhukhan, S. Kanungo, Phys. Rev. B **106** (12), 125112 (2022)
- (2) "Bulk photovoltaic effect in BaTiO_3 -based ferroelectric oxides: An **experimental** and theoretical study" S. Pal, S. Muthukrishnan, B. Sadhukhan, S. NV, D. Murali, P. Murugavel J. Appl. Phys. **129**, 084106 (2021)
- (3) "First-principles calculation of shift current in chalcopyrite semiconductor ZnSnP_2 " B. Sadhukhan, Y. Zhang, R. Ray, J. van den Brink Phys. Rev. Mat **4**, 064602 (2020)
- (4) "Electronic, magnetic, optical and thermoelectric properties of $\text{Ca}_{2-x}\text{Cr}_{1-x}\text{Ni}_x\text{OsO}_6$ double perovskites" B. Sadhukhan et al. RSC Advances **10** (27), 16179-16186 (2020).

Light-matter interaction in topological materials

- (1) "Effect of spin-lattice couplings on a Skyrmion multilayers $\text{Pd/Fe/Ir}(111)$ " B. Sadhukhan, A. Bergman, J. Hellsvik, A. Delin (Manuscript under preparation)
- (2) "Topological magnon in kagome spin spiral of YMn_6Sn_6 " B. Sadhukhan, A. Bergman, P. Thunström, M. Pereiro, O. Eriksson, A. Delin (Manuscript under preparation)
- (3) "Spin-lattice couplings in two-dimensional CrI_3 from first-principles computations" B. Sadhukhan, A. Bergman, Y. O. Kvashnin, J. Hellsvik, A. Delin Phys. Rev. B **105**, 104418 (2022)
- (4) Developing "UppASD package" code for atomistic spin-lattice simulation (<https://gitlab.com/UppASD/UppASD>)

Future research plan

Topology in electronic structure and transport

Sustainable transport via modern technologies

Light-matter interactions in Quantum magnets

Systems : Topological insulators, Weyl semimetals, multifold Fermions, Nodal line semimetals, Twisted bilayer systems

Topological properties and transport :

Anomalous Hall effect,
Planar Hall effect,
Circular photogalvanic effect,
Shift current response and anomalous photovoltaic effect,
Berry curvature dipole
Anomalous Nernst effect

Different probes :

Pressure, Strain, doping,
Electric and magnetic fields and many more

Systems : Topological magnon, Skyrmions, Spin spiral

Non-trivial transport :

Magnon Hall effect, Skyrmions Hall effect

Collaboration with Experimental and Theoretical team



Thankful to all my supervisors, collaborators,
parents and family



NORDITA



Thank you for your attention !!